Salt-penetrating and non-salt-penetrating tear faults in central Tarim Basin

qing bian[1] and Zhendong Wang[2]

[1]Sinopec
[2]Peking University

March 6, 2023

Abstract

We examined two tear faults, namely, Nos. 4 and 7 Faults, in Tarim Basin to investigate how a tear fault penetrates the salt layer. Using high-quality seismic data, we showed that No. 4 Fault penetrates the salt layer, whereas No. 7 Fault does not. We calculated the strata shortening data of Nos. 4 and 7 Faults. For No. 4 Fault, we observed shortening differences between the western and eastern sections in both the supra- and sub-salt strata, whereas for No. 7 Fault, we observed shortening differences only in the supra-salt strata. We demonstrated that under the action of thrusting, a tear fault could penetrate the salt layer if there is a shortening difference in the different positions of the sub-salt strata. A lack of shortening difference in the sub-salt strata implies that a tear fault cannot penetrate the salt layer, even though the sub-salt strata are deformed during thrusting.

Hosted file

957042_0_art_file_10758673_rqvg2y.docx available at https://authorea.com/users/591732/articles/627593-salt-penetrating-and-non-salt-penetrating-tear-faults-in-central-tarim-basin

Hosted file

957042_0_supp_10739823_rqkrt8.docx available at https://authorea.com/users/591732/articles/627593-salt-penetrating-and-non-salt-penetrating-tear-faults-in-central-tarim-basin

Salt-penetrating and non-salt-penetrating tear faults in central Tarim Basin

Qing Bian[1], **Zhendong Wang**[1,2,3]

[1]Petroleum Exploration and Production Research Institute, Sinopec, Beijing, China,

[2]National Energy Laboratory of Carbonate Oil and Gas, Sinopec, Beijing, China,

[3]Key Laboratory of Deep Geology and Resources, Sinopec, Beijing, China

Corresponding author: Qing Bian (bianqing.syky@sinopec.com)

Key Points:

- High-resolution seismic coherence maps were extracted clearly showing No. 4 Fault penetrated salt and No. 7 Fault terminated in salt
- Strata shortening data of Nos. 4 and 7 Faults were calculated to explain why No. 4 Fault can penetrate salt while No. 7 Fault cannot
- A lack of shortening difference in the sub-salt strata implies that a tear fault cannot penetrate the salt layer

Abstract

We examined two tear faults, namely, Nos. 4 and 7 Faults, in Tarim Basin to investigate how a tear fault penetrates the salt layer. Using high-quality seismic data, we showed that No. 4 Fault penetrates the salt layer, whereas No. 7 Fault does not. We calculated the strata shortening data of Nos. 4 and 7 Faults. For No. 4 Fault, we observed shortening differences between the western and eastern sections in both the supra- and sub-salt strata, whereas for No. 7 Fault, we observed shortening differences only in the supra-salt strata. We demonstrated that under the action of thrusting, a tear fault could penetrate the salt layer if there is a shortening difference in the different positions of the sub-salt strata. A lack of shortening difference in the sub-salt strata implies that a tear fault cannot penetrate the salt layer, even though the sub-salt strata are deformed during thrusting.

Plain Language Summary

Tear fault is a kind of steeply dip strike-fault caused by adjusting the displacement gap in the process of thrust. This paper deals with the problem of how deep a tear fault can extend downward. Due to the lack of deep data, previous studies on this problem mainly inferred indirectly from the evidence of outcrop scale. In this paper, high quality seismic data are used to clearly show whether two tearing faults, namely, Nos. 4 and 7 Faults, in the Tarim Basin can pass through the deep salt layer. Then, through the calculation of strata shortening, we prove that the sub-salt strata of No. 7 Fault did not have the original driving force to form the tear fault, while the sub-salt strata of No. 4 Fault were torn to form the tear fault.

1 Introduction

Tear faults are a common geological phenomenon on Earth and have been studied worldwide, for example, the Appalachian orogenic belt in West Virginia (Wheeler, 1980), Zagros orogenic belt in Iran (Jahani et al., 2017), north-eastern Maracaibo Basin in Venezuela (Escalona & Mann, 2006), and Niger Delta in Africa (Benesh et al., 2014). One aspect in the study of tear faults is evaluating how deep the tear fault can extend. In 1980, Wheeler's studied the downward progression of Parsons and Petersburg Lineaments in West Virginia, and assumed that they did not cut the basement. Wheeler cited evidence for surface mapping and gravity data; however, this evidence was indirect. In conclusion, Wheeler could not determine whether Parsons and Petersburg Lineaments passed through the deep detachment layer (Wheeler, 1980). Another study in the Burro Negro fault zone, based on outcrop and two-dimensional seismic data, suggested that the Burro Negro fault penetrated the salt layer (Escalona & Mann, 2006). However, outcrop observations do not provide adequate insights into subsurface conditions, and in practice, seismic interpretation is a blend of science and art (Jackson & Hudec, 2017) when the quality of seismic data is substandard. Based on outcrops, two-dimensional seismic data, and the focal depth of natural earthquakes, Jahani et al. (2017) suggested that a tear fault in the Zagros thrust belt did not penetrate the Hormuz salt layer; however, their calculation of the source depth of natural earthquakes may have contained errors. In general, the constriction on whether the tear fault can penetrate salt is mainly due to the poor quality of deep-earth data. Estimating the depth of a tear fault and evaluating why some tear faults cut through the deep salt (detachment layer) and others end at the salt layer are practically challenging.

This problem can effectively be solved using high-quality seismic data that can cover the development depth of a tear fault. In this study, we selected Nos. 4 and 7 tear faults in the Shuntuoguole Low Uplift, Tarim Basin, as the research subjects. Using high-resolution seismic data, we extracted the seismic coherence maps at different depths, which clearly indicated that No. 4 Fault penetrated salt and No. 7 Fault terminated in salt. We then explain why No. 4 Fault could cut through the salt as opposed to No. 7 Fault by analysing the strata shortening data.

2 Data and Methods

We used high-quality seismic data collected along Nos. 4 and 7 tear faults by Sinopec. Both the trace and bin spacings for the seismic cube are approximately 25 m. All seismic data were displayed in seconds, but the two-way-time-to-depth conversion was conducted using a velocity of 5500 m/s. In the map view, seismic coherence (Bahorich & Farmer, 1995) was used to image faults. Curvimetric and planimetric shortenings were calculated to evaluate the strata movement (Laubscher, 1961; Gonzalez-Mieres & Suppe, 2006).

3 Geological Setting

3.1 Tear faults in the Shuntuoguole Low Uplift

A series of tear faults has been observed in the Shuntuoguole Low Uplift. These faults are vertical, ranging in length from tens to hundreds of kilometres, but with a low slip distance. Sun et al. (2021) measured the slip distance of No. 5 Fault, which was between 200 and 1520 m. These tear faults can be classified into two systems according to the fault strike. The thrusting of the Katake Uplift resulted in the formation of Nos. 4, 6, 8, 12, 16, and southern No. 5 faults. The strike of these faults is NNE-SSW, perpendicular to the Tazhong No. 1 Fault. Another thrust-tear fault system was formed in the northwest region of the Shuntuoguole Low Uplift, including the northern part of No. 5 Fault and Nos. 7, 9, and 11 Faults. These faults are distributed in the NNW-SSE direction, perpendicular to the strike of the Luntai fault (Figure 1b). Considering the case of No. 5 Fault, Sun et al. (2021) studied the active stages of the tear faults. These tear faults began to form under regional compression during the middle Ordovician Period, and the entire thrust-tearing process lasted until the late Ordovician Period. By the beginning of the Silurian Period, the regional tectonic setting had become extensional (Sun et al., 2021).

3.2 Strata

Considering the tectonic setting, we focused on the Ordovician strata and those below it. Mudstones are deposited in the Yuertusi Formation (Deng et al., 2021). In the Xiaoerbulake Formation, the carbonate deposits are dominated by dolomite (Ji et al., 2020; Deng et al., 2019). Salt layers include the Wusonggeer Formation and the bottom of the Awatage Formation (Bian et al., 2022). The Shayilike Formation, comprising limestone, is sandwiched between salt layers. The supra-salt assemblage comprises dolomite, limestone, mudstone, and sandstone (Figure 1a).

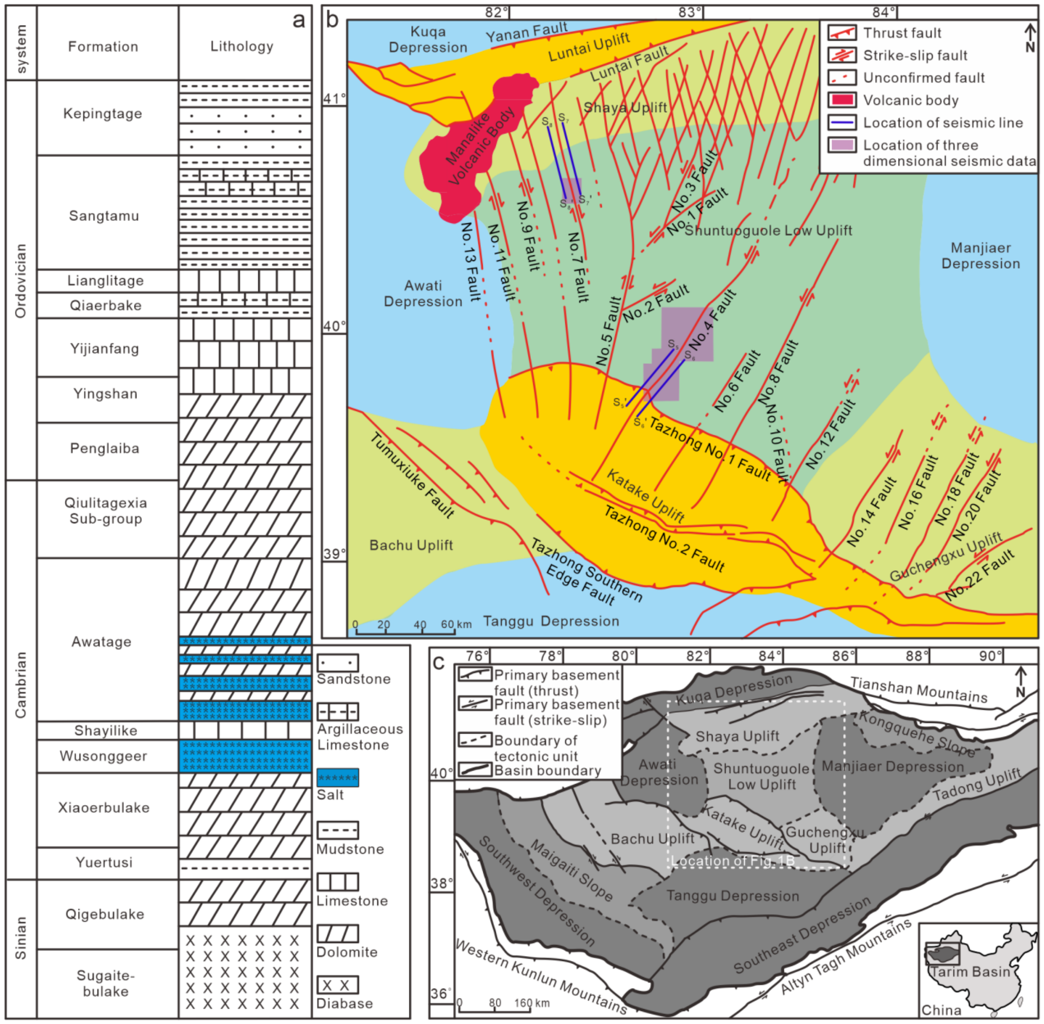

Figure 1. (a) The stratigraphy of Sinian, Cambrian, and Ordovician; (b) the distribution of faults in the Shuntuoguole Low Uplift (Figure 1c shows the locations). The faults are projected to the top of the Yijianfang Formation; (c) the structural units in the Tarim Basin.

4 Interpretation

4.1 Interpretation of No. 4 Fault

No. 4 Fault extends from the Katake Uplift to the Shuntuoguole Low Uplift. Its overall strike is NNE-SSW, perpendicular to that of the Tazhong No. 1 Fault. The fault strike is parallel to the southern parts of Nos. 5, 8, and 12 Faults (Figure 1b). We

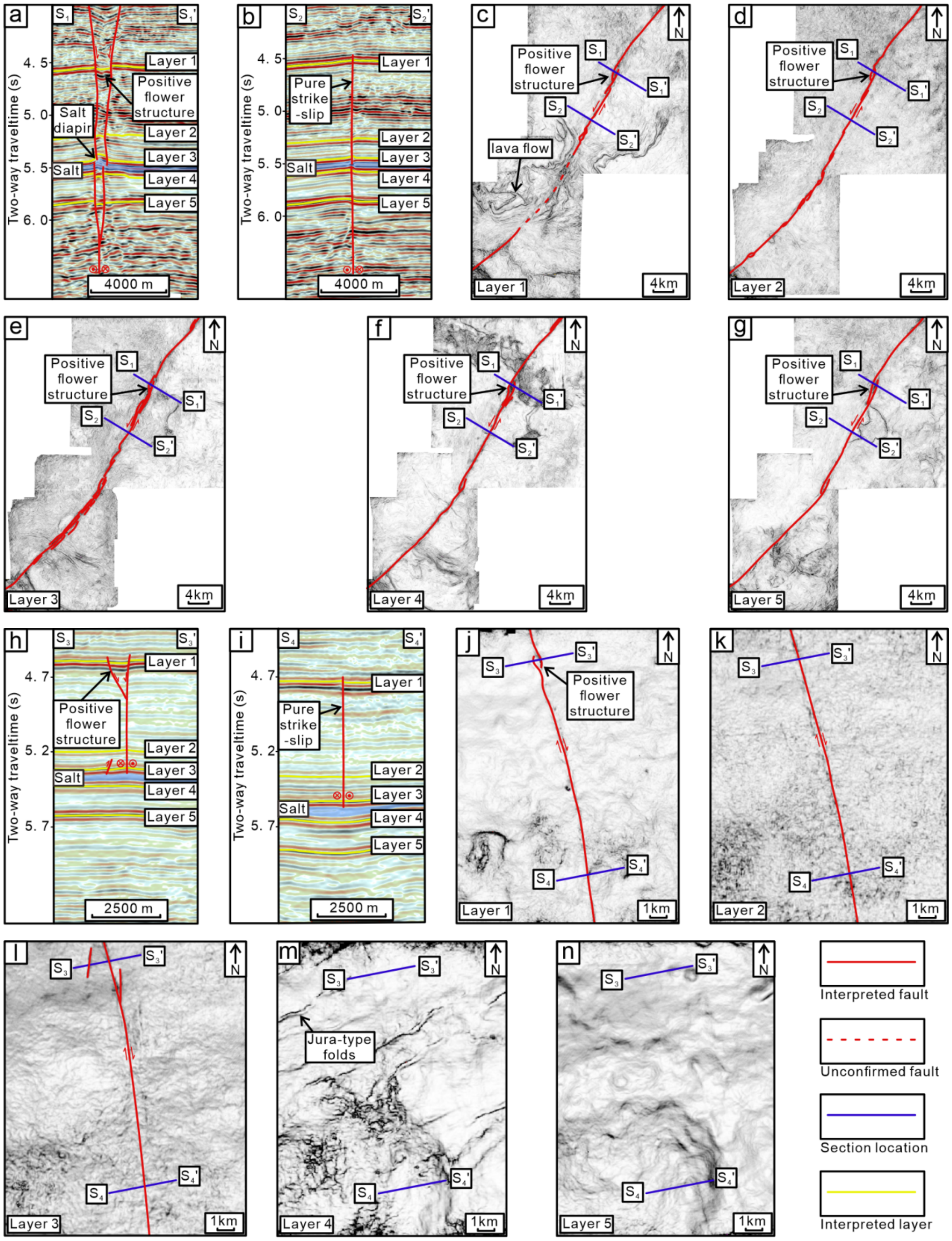

Figure 2. (a), (b), (h), (i) Interpretation for sections S_1, S_2, S_3, and S_4 (Figures 2 (c)-(g) and (j)-(n) show the locations); vertical exaggeration of the section = 2. (c)-(g) Interpretation of the top of the Yijianfang Formation, top of the Awatage Formation, top and bottom of the Wusonggeer Formation, and the bottom of Yuertusi Formation's coherence slices in No. 4 Fault. (j)-(n) Interpretation of the top of the Yijianfang

Formation, top of the Awatage Formation, top and bottom of the Wusonggeer Formation, and the bottom of Yuertusi Formation's coherence slices in No. 7 Fault. Figure 1b shows the locations of seismic data.

obtained seismic coherence maps of five layers of No. 4 Fault at various depths. Layers 1-5, respectively, cover the rigid strata above the salt, the top and bottom of the salt, and the rigid strata below the salt. Traces of the strike-slip fault can be observed in the five layers (Figures 2c–2g). For example, in section S_1, the fault develops a positive flower structure (Figure 2a). In the rigid layers, the structure style is consistent as the strata in the fault zone of layers 1, 2, and 5 collapsed. The seismic coherence maps show that the left-stepping fault stepover is present at this position (Figures 2c–2g). Accordingly, No. 4 Fault was evaluated to be a left-lateral fault (Fossen, 2010). Layer 3, the top layer of the salt, is convex in this position, forming a salt diapir, which is related to the low density and high rheology of salt (Bian et al., 2022). In general, the interpretation results of section S_1 (Figures 2c–2g), indicate that the sub-salt, salt, and supra-salt strata of No. 4 Fault are involved in a positive flower structure at this position. Section S_2 displays pure strike-slip, and notably, the fault penetrates the salt layer (Figure 2b). In summary, we determined that No. 4 Fault penetrated the salt layer.

4.2 Interpretation of No. 7 Fault

No. 7 Fault is an NNW-SSE trending tear fault developing in the northwest of the Shuntuoguole Low Uplift, belonging to the thrust-tear fault system in the northwest region of the Shuntuoguole Low Uplift (Figure 1b). Corresponding to the seismic coherence maps of No. 4 Fault, we extracted five seismic coherence maps of No. 7 Fault (Figures 2j–2n). No. 7 Fault is dominated by pure strike-slip, and only a small positive flower structure is observed in the northern part (Figure 2h). The positive flower structure can only be recognised in Figure 2j, and when it is folded down, it shows a linear distribution, as shown in Figure 2k. The positive flower structure shows a right-step distribution pattern (Figure 2j); thus, No. 7 Fault is evaluated as a right-lateral strike-slip fault (Fossen, 2010). No. 7 Fault is only shown in Figures 2j, k, l, and no trace of a fault is found in Figure 2m, which shows NEE-SWW-trending Jura-type folds. No fault was observed in sub-salt layer 5 (Figure 2n). In particular, No. 7 Fault only developed in the strata above the salt layer but not below it. Thus, No. 7 Fault did not penetrate the salt.

5 Calculation and Results

To determine why No. 4 Fault penetrates the salt and No. 7 Fault terminates above it, we must evaluate the cause of the tear fault. The tear fault is a strike-slip fault that mediates the difference in the strata displacement in different parts of the thrust system (Jackson & Hudec, 2017). Therefore, there was a difference in the strata shortening parallel to the thrust on the two sides of the tear fault. If the shortening of a block is consistent without a difference in displacement, no tear fault will be formed. If we can measure and compare the thrust shortening amount of the sub- and supra-salt strata on the two sides of the tear fault, we can determine why No. 4 Fault penetrates the salt while No. 7 Fault does not.

5.1 Strata shortening on both sides of No. 4 Fault

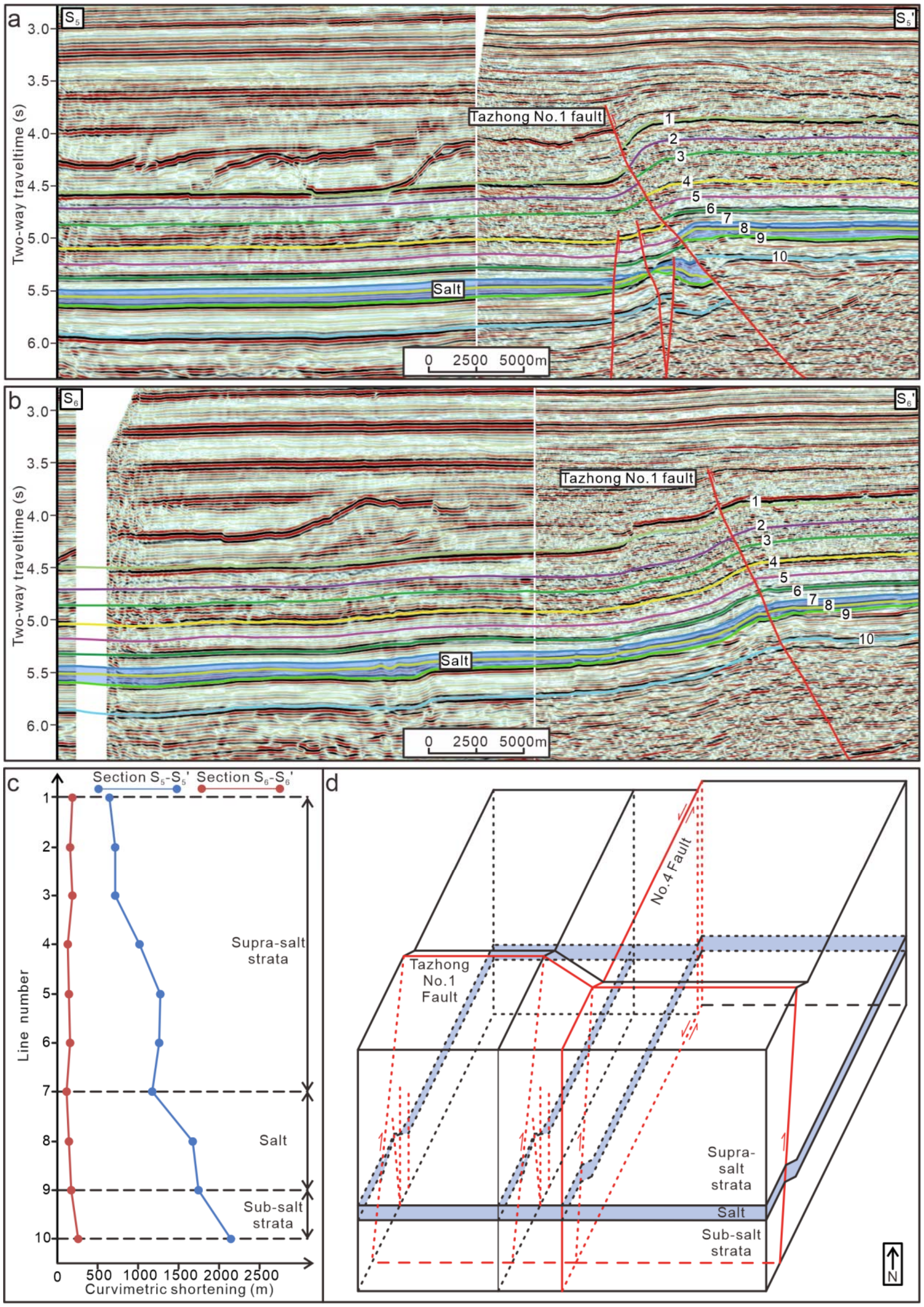

Figure 3. (a)-(b) Interpretation for sections S_5 and S_6 (Figure 1b shows the location); vertical exaggeration of the section = 2. (c) Curvimetric shortening in sections S_5, S_6. (d) Schematic diagram showing No. 4 Fault penetrating the salt.

We intercepted two seismic sections on the east and west sides of No. 4 Fault to elucidate formation shortening. The strike of the two seismic sections is parallel to that of No. 4 Fault, and the sections are approximately 5 km away from No. 4 Fault. Both sections cover the hanging wall and footwall of the Tazhong No.1 Fault. The lengths of the two sections are consistent at 45435.24 m. We chose 10 lines in two sections, including the supra-salt rigid, salt, and sub-salt strata. We measured and calculated the curvimetric shortening of the 10 lines on both sides of No. 4 Fault.

In section S_5 (Figure 3a), the Tazhong No. 1 Fault cuts through the strata above the salt, the salt layer, and strata below the salt, and obvious fault displacement is observed in the 10 interpreted lines. When the salt is cut through, plastic flow occurs, resulting in thinning and thickening of the salt. Simultaneously, three faults were derived from the footwall of the Tazhong No. 1 Fault, and were developed at great depths, namely, in the sub-salt strata, salt layer, and parts of the supra-salt strata. This indicates that in section S_5, the Tazhong No. 1 Fault has strong activity, and the supra-salt, salt, and sub-salt strata are all affected. In section S_6 (Figure 3b), the deformation is gentle compared with that in section S_5. Section S_6 shows that the fault displacement was small between the hanging wall and footwall of the Tazhong No. 1 Fault zone at this position. The thickness of the salt was stable. No secondary faults were observed in the footwall, indicating that the thrusting of the Tazhong No. 1 Fault does not cause obvious strata deformation at section S_6. In particular, the strata deformation on the western side of No. 4 Fault is more obvious than that on the eastern side.

The curvimetric shortening data shows differences on both sides of No. 4 Fault (Figure 3c). Overall, the curvimetric shortening of each line in section S_5 was greater than that in section S_6, including the sub-salt (lines 9 and 10), inter-salt (line 8), and supra-salt (lines 1–7) strata. Considering the supra-salt strata, the average curvimetric shortening of lines 1–7 in section S_5 is 972.84 m, and that in section S_6 is 152.26 m, with a difference of 820.58 m. Considering the sub-salt and inter-salt strata (lines 8–10), the average curvimetric shortening of lines 8–10 in section S_5 is 1855.20 m, and that in section S_6 is 193.28 m, with a difference of 1661.92 m.

Although the curvimetric shortening used here cannot accurately represent the actual amount of shortening (Gonzalez-Mieres & Suppe, 2006), under the same measurement standard, the curvimetric shortening reflects the difference in strata shortening. The western wall of No. 4 Fault caused a greater shortening amount, whereas its eastern wall had a smaller shortening amount. This difference explains why the strata at No. 4 Fault formed a tear fault. The shortening amounts of the supra- and sub-salt strata on both sides of No. 4 Fault are different; thus, both the supra- and sub-salt strata are torn to form faults, which explains why the tear of No. 4 Fault cuts through the salt (Figure 3d).

5.2 Strata shortening on both sides of No. 7 Fault

We obtained two seismic sections from the eastern and western sides of No. 7 Fault to measure the formation shortening. The strike of the two seismic sections was parallel to that of No. 7 Fault, and the sections were approximately 5 km away from No. 7 Fault. The lengths of the two sections are the same, namely, 45435.85 m. We chose 10 lines in two sections, covering the supra- to sub-salt strata.

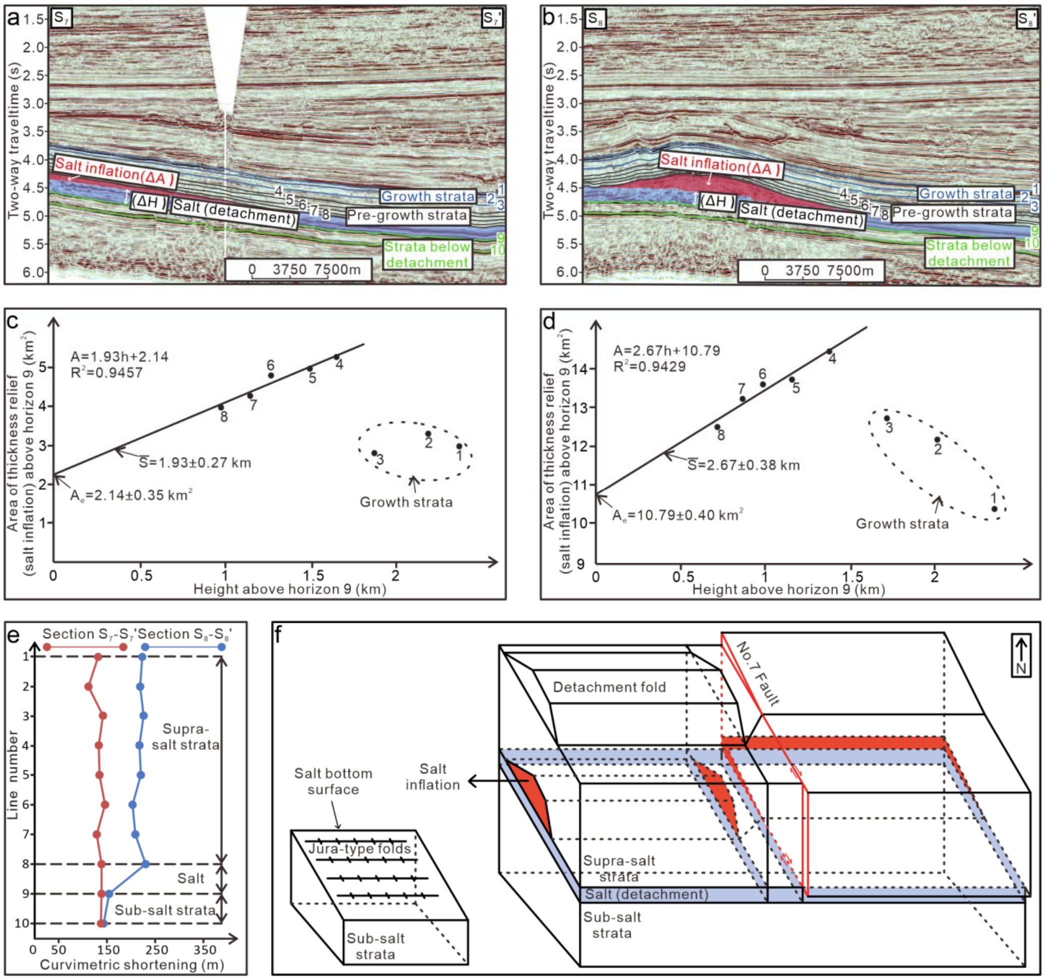

Figure 4. (a)-(b) Interpretation for sections S_7 and S_8 (Figure 1b shows the location); vertical exaggeration of the section = 2. (c)-(d) Area of relief graph for sections S_7 and S_8. (e) Curvimetric shortening in sections S_7 and S_8. (f) Schematic diagram showing that No. 7 Fault did not penetrate the salt.

Section S_7 shows that the strata are relatively gentle overall and inclined in the southeast direction; there is a slight thickening of salt (salt inflation) on the northwest side of section S_7 (Figure 4a). Comparatively, the salt is obviously thickened in section S_8, leading to the detachment fold in the supra-salt strata, whereas the sub-salt strata are inclined in the southeast direction owing to regional thrusting (Figure 4b).

Owing to the presence of detachment folds, planimetric shortening was calculated to recover the shortening of the supra-salt strata (lines 1–8). Line 9 was used as the reference. Simultaneously, we also collected the curvimetric shortening data. Using the sub-salt strata as the reference plane for measurement, we concluded that the average planimetric shortening (referring line 9) of the supra-salt strata in section S_7 is approximately 1.93 km (Figure 4c) and that in section H is 2.67 km (Figure 4d), with a difference of 0.74 km. The supra-salt strata on the eastern and western sides of No. 7 Fault have displacement differences owing to thrusting, and this difference led to the tearing of the supra-salt strata, forming a tear fault.

The average curvimetric shortening of the sub-salt strata (lines 9 and 10) in section S_7 is 138.32 m, whereas that in section S_8 is 148.50 m. This shows that although the strata were deformed beneath the salt, no significant displacement difference was observed between the eastern and western sides (Figure 4e). There is no incentive for the formation of tear faults in the sub-salt strata. This explains why No. 7 Fault ends above the salt (Figure 4f).

6 Discussion

In 1980, Wheeler's primary research objective was to determine whether Parsons and Petersburg Lineaments contained oil and gas (Wheeler, 1980). Similarly, for the Tarim Basin, the direct significance of this study was to evaluate the ability of the tear faults to connect with the deep source rock, namely, the Yuertusi Formation (Figure 1a). The NNE-SSW tear fault system is different from the NNW-SSE tear fault system. The comparison between the two tear fault systems showed that the NNW-SSE trending tear fault system did not penetrate salt; thus, it did not connect with deep source rocks, which is important evidence for geologists engaged in the study of the Tarim Basin.

Second, considering the development depth of tear faults, our results indicate that the extraction of high-precision layered seismic attributes has a direct effect. However, in the absence of good seismic data, the penetration of the tear fault into the salt can be indirectly determined through the calculation of supra- and sub-salt strata shortening. However, notably, if outcrop observations in an area with the development of tear faults show evidence of compressive deformation in the sub-salt strata, or the seismic interpretation of a single side of the tear fault shows evidence of deformation in the sub-salt strata, we cannot directly conclude that the tear fault penetrated the salt. Considering the example of No. 7 Fault, the sub-salt strata were compressed and deformed, and Jura-type folds appeared beneath the salt (Figure 2m). However, as no difference was observed in the shortening amount in different parts of the sub-salt strata, No. 7 Fault still did not penetrate the salt. Therefore, the most critical basis for evaluating whether a tear fault penetrates the salt is the difference in the thrust displacement amount of the sub-salt strata on both sides of the fault, rather than simply evaluating whether the sub-salt strata are compressed.

7 Conclusion

We extracted high-precision layered coherence maps in the seismic data covering two tear faults, namely, Nos. 4 and 7 Faults, in Shuntuoguole Low Uplift and found that No. 4 Fault penetrated the deep salt layer while No. 7 Fault did not. For No. 4

Fault, the strata shortening differences between the western and eastern sections exist in both the supra- and sub-salt strata, whereas for No. 7 Fault, the strata shortening differences only exist in the supra-salt strata. This result indicated that a tear fault cannot penetrate the salt layer when there is no shortening difference in the sub-salt strata, even though the sub-salt strata can be deformed during thrusting.

Acknowledgments

This study is based upon work of the Basic Research Program that financially supported by National Natural Science Foundation of China (No. U21B2063), and by Sinopec under project number P22125. Many thanks to the Northwest Oilfield Company of Sinopec for the supplement of data.

Open Research

Data Availability Statement

The seismic data supporting this research are owned by Sinopec, with commercial restrictions, and are not accessible to the public or research community. The seismic profiles used in this study is available at https://doi.org/10.6084/m9.figshare.22197646.v1.

References

Bahorich, M., and Farmer, S., 1995, 3-D seismic discontinuity for faults and stratigraphic features; the coherence cube: The Leading Edge, v. 14, p. 1053-1058.

Benesh, N.P., Plesch, A., and Shaw, J.H., 2014, Geometry, kinematics, and displacement characteristics of tear-fault systems: An example from the deep-water Niger Delta: AAPG Bulletin, v. 98, p. 465-482, doi:10.1306/06251311013.

Bian, Q., Deng, S., Lin, H., and Han, J., 2022, Strike-slip salt tectonics in the Shuntuoguole Low Uplift, Tarim Basin, and the significance to petroleum exploration: Marine and Petroleum Geology, v. 139, 105600.

Deng, S., Li, H., Zhang, Z., Zhang, J., Yang, X., 2019, Structural characterization of intracratonic strike-slip faults in the central Tarim Basin: AAPG Bulletin, v. 103, p. 109-137.

Deng, Q., Zhang, H., Wang, H., Wei, Z., Cheng, B., Li, S., Wang, Y., Faboya, O.L., and Liao, Z., 2021, Organic Matter Accumulation Mechanism in the Lower Cambrian Strata from Well Luntan 1 in the Tarim Basin, NW China: Geofluids, v. 4, p. 1-13.

Escalona, A., and Mann, P., 2006, Tectonic controls of the right-lateral Burro Negro tear fault on Paleogene structure and stratigraphy, northeastern Maracaibo Basin: AAPG Bulletin, v. 90, p. 479-504.

Fossen, H., 2010, Structural Geology: Cambridge, Cambridge University Press.

Gonzalez-Mieres, R., and Suppe, J., 2006, Relief and shortening in detachment folds: Journal of Structural Geology, v. 28, p. 1785-1807, doi:10.1016/j.jsg.2006.07.001.

Jackson, M.P.A., and Hudec, M.R., 2017, Salt tectonics: principles and practice: Cambridge, Cambridge University Press.

Jahani, S., Hassanpour, J., Mohammadi-Firouz, S., Letouzey, J., Frizon de Lamotte, D., Alavi, A.S., and Soleimany, B., 2017, Salt tectonics and tear faulting in the central part of the Zagros Fold-Thrust Belt, Iran: Marine and Petroleum Geology, v. 86, p. 426-446, doi:10.1016/j.marpetgeo.2017.06.003.

Ji, T., Yang, W., Pu, R., and Wu, X., 2020, Research on the lithofacies and paleogeography of the lower Cambrian Xiaoerbulake Formation in the northern Tarim Basin, northwestern China: Canadian Journal of Earth Sciences, v. 57, p. 1463-1477.

Kang, Y., and Kang, Z., 1996, Tectonic evolution and oil and gas of Tarim Basin: Journal of Southeast Asian Earth Sciences, v. 3, p. 317-325.

Laubscher, H.P., 1961, Die Fernschubhypothese der Jurafaltung: Eclogae Geologicae Helvetiae, v. 54, p. 221-282.

Sun, Q., Fan, T., Gao, Z., Wu, J., Zhang, H., Jiang, Q., Liu, N., and Yuan, Y., 2021, New insights on the geometry and kinematics of the Shunbei 5 strike-slip fault in the central Tarim Basin, China: Journal of Structural Geology, v. 150, 104400.

Wheeler, R.L., 1980, Cross-Strike Structural Discontinuities: Possible Exploration Tool for Natural Gas in Appalachian Overthrust Belt: AAPG Bulletin, v. 64, p. 2166-2178, doi:10.1306/2F91975B-16CE-11D7-8645000102C1865D.